

中文摘要

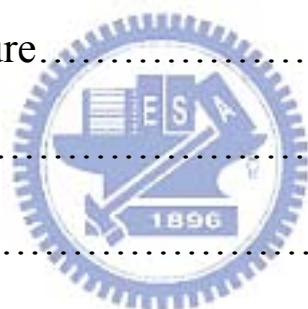
我們利用穿透式電子顯微鏡研究鐵-8.8 鋁-30 錳-6 鉻-1.0 矽-1.0 碳合金之相變化。在淬火狀態下，此合金的顯微組織為單一的沃斯田鐵相。當此合金在 550 至 1000°C 時效熱處理後隨溫度增加，其相變化過程為 $((\text{Fe, Mn, Cr})_7\text{C}_3 + \text{D0}_3) \rightarrow ((\text{Fe, Mn, Cr})_7\text{C}_3 + \text{B2}) \rightarrow ((\text{Fe, Mn, Cr})_7\text{C}_3 + \alpha) + \gamma \rightarrow ((\text{Fe, Mn, Cr})_7\text{C}_3 + \gamma) \rightarrow \gamma$ ，可以明顯地發現沒有 $(\text{Fe, Mn, Cr})_{23}\text{C}_7$ 碳化物的產生在此成份的合金。這樣的相變化過程與之前被研究的鐵-8.8 鋁-30 錳-6 鉻-1.0 碳合金的相變化過程非常不一樣。此外，650°C 時的 B2 相擁有比在 750°C 時的 α 相較多的矽含量，因此，造成在 650°C 時效處理所產生的 D0_3 相會比在 750°C 時效處理還大。

Abstract

The Phase transformations in the Fe-8.8Al-30Mn-6Cr-1.0Si-1.0C alloy have been examined by means of transmission electron microscopy. In the as-quenched condition, the microstructure of the alloy was the single phase austenite. When the as-quenched alloy was aged at temperatures ranging from 550 to 1000°C, the phase transformation sequence as the aging temperature increased was found to be $((\text{Fe,Mn,Cr})_7\text{C}_3+\text{D0}_3) \rightarrow ((\text{Fe,Mn,Cr})_7\text{C}_3+\text{B2}) \rightarrow ((\text{Fe,Mn,Cr})_7\text{C}_3+\alpha) + \gamma \rightarrow ((\text{Fe,Mn,Cr})_7\text{C}_3 + \gamma) \rightarrow \gamma$, in which no $(\text{Fe,Mn,Cr})_{23}\text{C}_7$ carbides could be found in the present alloy. These results are quite different from that observed in the Fe-8.8Al-30Mn-6Cr-1.0C alloy. Besides, since the B2 phase present at 650°C contains much more silicon than the ferrite phase present at 750°C, the size of the D0_3 domains was much larger than that of the alloy aged at 750°C and then quenched.

Contents

Abstract(Chinese).....	1
Abstract(English).....	2
Contents.....	3
List of Figures.....	4
List of Tables.....	6
Introduction.....	7
Experimental Procedure.....	10
Results.....	12
Discussion.....	19
Conclusions.....	23
References.....	25



List of Figures

Figure 1. (a) an optical micrograph of the as-quenched alloy.

Electron micrographs of the as-quenched alloy, (b) BF,

(c) and (d) two SADPs taken from the austenite matrix.

The foil normals are $[011]$ and $[111]$, respectively...29

Figure 2. Electron micrographs of the alloy aged at 550°C for

6 hours, (a) BF, (b) and (c) two SADPs taken from a

mixed region covering the fine κ' -carbides and the

austenite matrix. The zone axes are $[001]$ and $[011]$,

respectively. (hkl = austenite matrix; hkl = κ' -

carbide).....31

Figure 3. Electron micrographs of the alloy aged at 550°C for

72 hours, (a) and (b) BF, (c) through (e) are three

SADPs taken from the precipitate marked as A in (b).

The foil normals are $[1210]$, $[1100]$ and $[0001]$,

respectively. (f) an SADP taken from the area marked

as B in (b). The zone axe is $[011]$. ($hkl = D0_3$)(g) and

(h) are (111) and (200) $D0_3$ DF,

respectively.....33

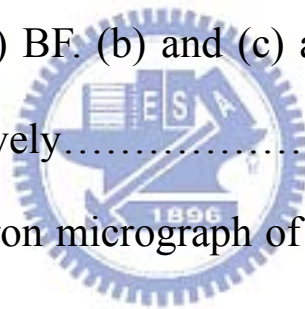
Figure 4. An SEM electron micrograph of the alloy aged at 550 °C for 240 hours.....37

Figure 5. Electron micrographs of the alloy aged at 650°C for 72 hours, (a) BF. (b) and (c) are (111) and (200) D_{03} DF, respectively.....38

Figure 6. Electron micrographs of the alloy aged at 750°C for 24 hours, (a) BF. (b) and (c) are (111) and (200) D_{03} DF, respectively.....40

Figure 7. (a) BF electron micrograph of the alloy aged at 850°C for 2 hours and (b) BF electron micrograph of the alloy aged at 850°C for 6 hours.....42

Figure 8. BF electron micrograph of the alloy aged at 1100°C for 2 hours.....43



List of Tables

Table I. Chemical Compositions of the Phases Revealed By an Energy-Dispersive Spectrometer (EDS).....	44
---	----



Introduction

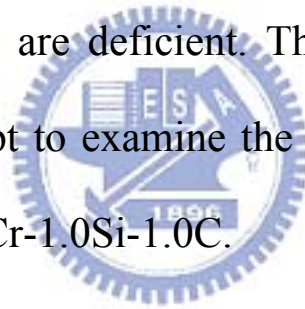
Phase transformations in the Fe-Al-Mn-C alloys, prepared by conventional casting process or by rapid solidification process, have been extensively studied by many workers [1-15]. These studies have shown that in the as-quenched or in the as-solidified condition, the microstructure of the alloy with a chemical composition in the range of Fe-(8-11) wt.% Al-(28-35) wt.% Mn-(0.8-1.6) wt.% C was single-phase austenite (γ). After being aged at temperatures ranging from 500°C to 750°C, the $(\text{Fe,Mn})_3\text{AlC}$ carbides having an $L'1_2$ -type structure started to precipitate not only within the austenite matrix but also on the γ/γ grain boundaries. For convenience, the κ' -carbide and κ -carbide were used to represent the $(\text{Fe,Mn})_3\text{AlC}$ carbide formed within the austenite matrix and on the γ/γ grain boundaries, respectively [6]. After prolonged aging within this temperature range, the κ -carbide grew into the adjacent austenite grains through a $\gamma \rightarrow \alpha$ (ferrite) + κ -carbide reaction, or a $\gamma \rightarrow \alpha + \kappa\text{-carbide} + \beta\text{-Mn}$ reaction [5,6,15].

In order to improve the high-temperature oxidation resistance and corrosion resistance, silicon and chromium have been added to the Fe-Al-Mn-C alloys [2,17-21]. Based on their studies, it can be generally concluded that the silicon and chromium additions could achieve these results. In addition, the effects of silicon on the microstructures of the Fe-Al-Mn-C alloys have also been examined principally by either optical microscopy or scanning electron microscopy [2,22,23]. It was proposed that the addition of silicon would enhance the formation of the ferrite phase in the Fe-Al-Mn-C alloys. Recently, we performed transmission electron microscopy observations on the phase transformations in Fe-7.8Al-29.5Mn-1.5Si-1.05C and Fe-9.8Al-28.6Mn-0.8Si-1.0C alloys [25-27]. Consequently, we found that when the alloys were aged at temperatures ranging from 550°C to 850°C, both of the D0₃ and B2 phases could be observed and no evidence of the ferrite phase could be detected. This result is quite different from that observed by other workers in the Fe-Al-Mn-Si-C alloys [2,22,23].

Furthermore, the phase transformation of an

Fe-8.8Al-30Mn-6Cr-1C alloy has also been examined by our workers [32]. When the Fe-8.8Al-30Mn-6Cr-1C alloy was aged at temperatures ranging from 500 °C to 800 °C, the phase transformation sequence as the temperature increased was found to be $\gamma + \kappa'$ -carbide $\rightarrow \gamma + (\text{Fe,Mn,Cr})_{23}\text{C}_6 \rightarrow \gamma + (\text{Fe,Mn,Cr})_7\text{C}_3$.

However, information concerning the microstructural development of Fe-Al-Mn-C alloys with the additions of both silicon and chromium are deficient. Therefore, the purpose of this work is an attempt to examine the phase transformation of the Fe-30Mn-8.8Al-6Cr-1.0Si-1.0C.



Experimental Procedure

(A) Alloy Preparation

The alloy, Fe-30wt.%Mn-8.8wt.%Al-6.0wt.%Cr-1.0wt.%Si-1.0wt.% C, was prepared in an air induction furnace by using electrolytic iron (99.5%), electrolytic aluminum (99.7%), electrolytic manganese (99.9%), pure carbon powder, electrolytic chromium (99.9%) and ferrosilicon. After being homogenized at 1250°C for 24 hours under a protective argon atmosphere, the ingot was hot-forged and cold-rolled to a final thickness of 3.0 mm. The sheets were subsequently austenitized at 1150°C for 1 hour and then quenched into room temperature water. The aging processes were performed at the temperatures ranging from 550°C to 1000°C for various times in a vacuum furnace and then quenched into water rapidly.

(B) Microstructure Observations and Diffraction Analyses

(1) Optical Microscopy (OM)

The optical microscopic specimens were prepared as the following steps: sectioning, mounting, rough polishing, fine

polishing and finally etching with 10% nital.

(2) Transmission Electron Microscopy (TEM)

The transmission electron microscopic specimens were prepared by means of a double jet electropolisher with an electrolyte of 10% perchloric acid, 15% acetic acid, 75% ethanol. The polishing temperature was kept in the range from -30°C to -20°C and the current density was kept in the range from 3.5 to $4 \times 10^4 \text{ A/m}^2$. Electron microscopy was performed on a JEOL-2000FX scanning transmission electron microscope (STEM) operating at 200kV.

(3) Scanning Electron Microscopy (SEM)

The samples of scanning electron microscopy were obtained similar to STEM samples. Scanning electron microscopy was performed on a JEOL- 6500FX Field-emission SEM operating at 15kV. The SEM microscope was equipped with an energy-dispersive X-ray spectrometer (EDS) for chemical analysis and distribution. Quantitative analyses of elemental concentrations for Fe, Al, Mn, Cr and Si were made with the aid of a Cliff-Lorimer ratio Thin Section method.

Results

Figure 1(a) is an optical micrograph of the alloy after being solution heat-treated at 1150°C for 1 hour and then quenched into water. It reveals a single austenite phase with annealing twins. Figure 1(b) is a bright-field (BF) electron micrograph of the as-quenched alloy. Figures 1(c) and (d) are selected-area diffraction patterns (SADPs) taken from the matrix in Figure 1(b). The zone axes are [011] and [111], respectively. It is seen that in addition to the reflection spots corresponding to the disordered austenite phase (γ), no extra spots could be observed. This result indicates that the microstructure of the as-quenched alloy was single austenite phase.

Figure 2(a) is a BF electron micrograph of the alloy after being aged at 550°C for 6 hours, showing that fine precipitates were formed within the austenite matrix. Figures 2(b) and 2(c) are two SADPs taken from the austenite matrix and its surrounding fine precipitates. The zone axes of the austenite phase are [001] and [011], respectively. Compared to the previous studies in the Fe-Al-Mn-C alloys [6-9], it is clear that

the fine precipitates are $(\text{Fe,Mn})_3\text{AlC}$ carbides (κ' -carbide) having an L'_{12} -type structure. In Figure 2(b), it is also seen that the satellites lying along $\langle 001 \rangle$ reciprocal lattice direction about the (200) and (220) reflections could be observed. On the basis of the above observations, it is concluded that the microstructure of the present alloy aged at 550°C for 6 hours was the austenite phase containing fine κ' -carbides.

Transmission electron microscopy examinations indicated that when the as-quenched alloy was aged at 550°C for a period of time less than 24 hours, no precipitates could be detected on the austenite grain boundaries. However, when the aging time was longer than 36 hours, another type precipitates started to occur on the grain boundaries. An example is shown in Figure 3. Figures 3(a) and 3(b) are BF electron micrographs of the alloy aged at 550°C for 72 hours, showing that some plate-like precipitates could be observed on the grain boundaries. Figures 3(c) through (e) are three SADPs taken from the plate-like precipitate marked as “A” in Figure 3(b). By analyzing these values of interplanar spacings and angles between reciprocal

vectors in these SADPs, it was determined that the plate-like precipitate is $(\text{Fe,Cr,Mn})_7\text{C}_3$ carbide having hexagonal cubic primitive structure with lattice parameters $a=1.0735\text{nm}$ and $c=0.609\text{nm}$. The crystallographic normals shown in Figures 3(c) through (e) are $[1210]$, $[1100]$ and $[0001]$, respectively. Figure 3(f), an SADP taken from the area marked as “B” in Figure 3(b), shows that the crystal structure is D0_3 phase [22-23, 25-27]. Figures 3(g) and 3(h), (111) and (200) D0_3 DF electron micrograph of the same area as in Figure 3(b), show the presence of large D0_3 domains. This indicates that the D0_3 phase was existent at the aging temperature. Therefore, the microstructure present on the grain boundaries was the mixture of $(\text{Fe,Cr,Mn})_7\text{C}_3$ carbide and D0_3 phase. With increasing the aging time at 550°C the precipitation of $[(\text{Fe,Cr,Mn})_7\text{C}_3 + \text{D0}_3]$ grew into the adjacent austenite grains. A typical example is shown in Figure 4, which is an SEM electron micrograph of the alloy aged at 550 for 240 hours. Based on the above observations, it is concluded that the microstructure of present alloy in the equilibrium stage at 550°C was a mixture of

$((\text{Fe,Cr,Mn})_7\text{C}_3 + \text{D0}_3)$ phases. Transmission electron microscopy observations revealed that the $((\text{Fe,Cr,Mn})_7\text{C}_3 + \text{D0}_3)$ phases could be detected up to 625°C .

When the alloy was aged at 650°C for 3 hours and then quenched, the microstructure is similar to the alloy aged at 550°C for short times. It was the austenite phase containing fine κ' -carbides and no precipitates could be found on the grain boundaries. Figure 5(a) is a BF electron micrograph of the alloy aged at 650°C for 72 hours. Analyses by the SADP indicated that these two phases were also $(\text{Fe,Cr,Mn})_7\text{C}_3$ and D0_3 , respectively. Therefore, it is likely to conclude that the stable microstructure of the alloy at 650°C was also the mixture of $((\text{Fe,Cr,Mn})_7\text{C}_3 + \text{D0}_3)$ phases. However, the (111) D0_3 DF electron micrograph showed that only extremely fine D0_3 domains were present within the matrix, whereas the (200) D0_3 DF electron micrograph revealed that the whole plate were bright in contrast as indicated in Figures 5(b) and 5(c). This indicates that the microstructure of the matrix present at 650°C should be B2 phase and the extremely fine D0_3 domains were

formed during quenching process from 650 °C to room temperature by a B2→D0₃ continuous ordering transition[28,29]. On the basis of the above observations, it is concluded that the stable microstructure of the alloy at 650 °C should be the mixture of (Fe,Cr,Mn)₇C₃ and B2 phase. This indicates that a ((Fe,Cr,Mn)₇C₃ +D0₃) → (B2+(Fe,Cr,Mn)₇C₃) transition has occurred between 625 °C and 650 °C.

When the alloy was aged at 750 °C for 3 hours and then quenched, the microstructure is similar to that of the as-quenched alloy. It reveals a single austenite phase with annealing twins and no precipitates could be examined. However, after prolonged aging time at this temperature, two types of precipitates could be observed on the grain boundaries and no precipitates could be detected with the austenite matrix. An example is shown in Figure 6. Figure 6(a) is a BF electron micrograph of the alloy aged at 750 °C for 24 hours and then quenched. Analyses of the particle marked as “C” and “D” showed that the microstructures of these two particles were also (Fe,Cr,Mn)₇C₃ and α phase, respectively. However, as shown in

Figures 6(b) and 6(c), the (111) and (200) DF electron micrographs revealed that only extremely fine $D0_3$ domains and small B2 domains were present within the $D0_3$ phase. This indicates that a $\alpha \rightarrow B2 \rightarrow D0_3$ continuous ordering transition has occurred during quenching within the α phase [25-27]. It means that the stable microstructure of the present alloy at 750 °C was a mixture of austenite (γ) phase, $(Fe,Cr,Mn)_7C_3$ carbide and ferrite (α) phase.

When the alloy was aged at 850°C for 2 hours and then quenched, it reveals that only $(Fe,Cr,Mn)_7C_3$ carbide occurred on the austenite grain boundaries, as shown in Figure 7(a). Figure 7(b), a BF electron micrograph of the alloy aged at the same temperature for a long period of time, indicates that in addition to the grown $(Fe,Cr,Mn)_7C_3$ carbides, no other precipitates could be detected on the grain boundaries. Therefore, the stable microstructure of the present alloy aged at 850°C was a mixture of $(\gamma + (Fe,Cr,Mn)_7C_3)$ phases. Transmission electron microscopy examinations revealed the stable microstructure of the $(\gamma + (Fe,Cr,Mn)_7C_3)$ phases could be preserved up to a

temperature of 950°C. However, when the alloy was aged at 1000°C for various times and then quenched, only austenite phase could be detected in the present alloy, as shown in Figure 8. It is similar to that observed in the alloy after being solution heat-treated at 1150°C. This indicates that microstructure of present alloy aged at 1000°C or above should be the single austenite phase.



Discussion

Based on the above experimental results, some discussions are appropriate. When the alloy was aged at temperatures ranging from 550 °C to 1000 °C, the phase transformation sequence was found to be $((\text{Fe,Cr,Mn})_7\text{C}_3+\text{D0}_3) \rightarrow ((\text{Fe,Cr,Mn})_7\text{C}_3+\text{B2}) \rightarrow ((\text{Fe,Cr,Mn})_7\text{C}_3+\alpha+\gamma) \rightarrow ((\text{Fe,Cr,Mn})_7\text{C}_3+\gamma) \rightarrow \gamma$. This result is quite different from that in our previous studies, in which neither $\alpha \rightarrow \text{B2} \rightarrow \text{D0}_3$ nor $\text{B2} \rightarrow \text{D0}_3$ continuous ordering transition could be found in Fe-8.8Al-30.0Mn-6.0Cr-1.0C alloy [32]. In order to clarify the apparent difference, an STEM-EDS study was undertaken. The average concentrations of the alloying elements were obtained by analyzing at least ten different EDS spectra of each phase. EDS with a thick-window detector is limited to detect the elements of atomic number of 11 or above; therefore, carbon cannot be examined by this method. The results are summarized in Table I. It is clearly seen in Table I that the concentrations of both the aluminum and silicon in the $(\text{Fe,Cr,Mn})_7\text{C}_3$ carbides are

much less than that in the α , B2 or D0₃ phase, and the reverse result is obtained for the concentrations of the manganese and chromium. It is well-known that manganese and carbon are austenite former in the Fe-Mn-Al-C quaternary alloy systems [38, 39], and the carbon content in the (Fe,Cr,Mn)₇C₃ carbide is much higher than that in the present alloy. Therefore, it is reasonable to believe that along with the precipitation of the (Fe,Cr,Mn)₇C₃ carbides, the surrounding austenite phase would be lacked in manganese as well as carbon, and enriched in aluminum and silicon. The austenite phase in the vicinity of the (Fe,Cr,Mn)₇C₃ carbides would become unstable and readily transform into the ferrite phase. Subsequently, it is likely to expect that the $\alpha \rightarrow B2 \rightarrow D0_3$ and $B2 \rightarrow D0_3$ continuous ordering transition would occur during quenching from the aging temperature of 750 °C and 650 °C in the present alloy, respectively, as shown in Figures 5 and 6. However, in the Fe-Al binary alloys, a $\alpha \rightarrow B2 \rightarrow D0_3$ continuous ordering transition could be just occurred as containing above 25 at.% aluminum [28, 29]. It is clear in Table 1 that the aluminum content of the

ferrite phase at 750°C is only 11.05 wt.% or 20.00 at.%. The reason why a $\alpha \rightarrow B2 \rightarrow D0_3$ continuous ordering transition could be observed is silicon addition in the present alloy. From our previous studies in Fe-Al-Mn-Si-C alloys, we have shown that the addition of silicon would lead the $\alpha \rightarrow B2 \rightarrow D0_3$ continuous ordering transition to occur[25-27]. Therefore, it is reasonable to expect that owing to the enrichment of silicon, a $\alpha \rightarrow B2 \rightarrow D0_3$ and $B2 \rightarrow D0_3$ continuous ordering transition would occur during quenching from 750°C and 650°C in the present alloy.

Furthermore, when the present alloy was aged at 750°C or 650°C and then quenched, the $D0_3$ domains would be formed during quenching by a $B2 \rightarrow D0_3$ continuous ordering transition. However, as compared Figure 5(b) with 6(b), it is obvious that the size of $D0_3$ domains in Figure 5(b) is much larger than that in 6(b). Based on our previous studies [25-27], it was also found that the addition of silicon would expand the $D0_3$ phase region. This means that the $B2 \rightarrow D0_3$ transition temperature would be increased with increasing the addition of silicon. As shown in Table I, it is clearly seen that the silicon concentration of the B2

phase at 650°C is higher than that of the ferrite phase at 750°C. Thus, when the present alloy was aged at 650°C and then quenched, the B2→D0₃ ordering transition would occur at higher temperature, which results in the larger size of D0₃ domains.

Finally, it is interesting to note that the precipitation of (Fe,Cr,Mn)₂₃C₆ carbides was absent in the present alloy. This is contrary to that found in the previous Fe-8.8Al-30.0Mn-6.0Cr-1.0C alloy [32]. Compared to our previous Fe-8.8Al-30.0Mn-6.0Cr-1.0C alloy, in addition to contain 1.0 wt.% silicon in the present alloy, both alloys were composed of similar compositions. Therefore, it is possible to suggest that the addition of silicon to the Fe-Al-Mn-Cr-C alloys would inhibit the precipitation of (Fe,Cr,Mn)₂₃C₆ carbides.

Conclusions

In the present study, the phase transformations in the Fe-8.8Al-30Mn-6Cr-1.0Si-1.0C alloy have been examined by transmission electron microscopy.

- (1). In the as-quenched condition, the microstructure of the present alloy was the single phase austenite.
- (2). When the as-quenched alloy was aged at temperature ranging from 550 to 1000°C, the phase transformation sequence as the aging temperature increased was found to be $((\text{Fe},\text{Mn},\text{Cr})_7\text{C}_3+\text{D0}_3) \rightarrow ((\text{Fe},\text{Mn},\text{Cr})_7\text{C}_3+\text{B2}) \rightarrow ((\text{Fe},\text{Mn},\text{Cr})_7\text{C}_3+\alpha) + \gamma \rightarrow ((\text{Fe},\text{Mn},\text{Cr})_7\text{C}_3+\gamma) \rightarrow \gamma$
- (3). When the as-quenched alloy was aged at 650°C or 750°C and then quenched, the D0₃ domains would be formed during quenching by a B2→D0₃ continuous ordering transition. Since B2 phase present at 650°C contains much more silicon than the ferrite phase present at 750°C, then the size of the D0₃ domains was much larger than that of the alloy aged at 750°C and then quenched.

(4). When the as-quenched alloy was aged at temperatures ranging from 550 to 1000°C, the $(\text{Fe,Cr,Mn})_{23}\text{C}_6$ carbides were always observed in the Fe-Al-Mn-Cr-C alloys. However, no $(\text{Fe,Cr,Mn})_{23}\text{C}_6$ carbides could be found in the present alloy. Therefore, it is suggested that the addition of silicon to the Fe-Al-Mn-Cr-C alloys would inhibit the precipitation of $(\text{Fe,Cr,Mn})_{23}\text{C}_6$ carbides.



References

1. G. L. Kayak, Met. Sci. Heat Treat. 11(2) (1969) 95.
2. D. J. Schmatz, Trans. ASM. 52 (1960) 898.
3. C. N. Hwang, C. Y. Chao and T. F. Liu, Scripta Matall. 28 (1993) 263.
4. S. C. Chang and Y. H. Hsiau, J. Mater. Sci. 24 (1989) 1117.
5. G. S. Krivonogov, M. F. Alekseyenko and G. G. Solov'yeva, Phys. Met. Metall. 39(4) (1975) 86.
6. K. H. Han and W. K. Choo, Metall. Trans. A. 20A (1989) 205.
7. T. F. Liu. and C. M. Wan, Strength Met. Alloys 1 (1986) 423.
8. N. A. Storchak and A. G. drachinskaya, Phys. Met. Metall. 44(2) (1977) 123.
9. K. Sato, K. Tagawa and Y. Inoue, Scripta Metall. 22(6) (1988) 899.
10. K. Sato, K. Tagawa and Y. Inoue, Metall. Trans. A. 21A (1990) 5.
11. K. H. Han, J. C. Yoon and W. K. Choo, Scripta Metall. 20(1)

- (1985) 33.
- 12.K. H. Han, W. K. Choo and D. E. Laughlin, Scripta Metall.
22(12) (1988) 1873.
- 13.K. Sato, K. Tagawa and Y. Inoue, Mater. Sci. Eng. A111
(1989) 45.
- 14.J. E. Krzanowski, Metall. Trans. A. 19(A), 1873, (1988).
- 15.W. K. Choo and K. H. Han, Metall. Trans. A, 16A (1985) 5.
- 16.S. K. Banerji, Met. Prog. Apr. (1978) 59.
- 17.R. Wang and F. H. Beck, Met. Prog. Mar. (1983) 72.
- 18.U. Bernabai, G. A. Capuano, A. Dang and F. Felli, Oxid. Met. 33
(1990) 809.
- 19.J. P. Sauer, R. A. Rapp and J. P. Hirth, Oxid. Met. 18 (1982)
285.
- 20.J. C. Garcia, N. Rosas and R. J. Rioja, Met. Prog. Aug. (1982)
47.
- 21.J. S. Dunning, M. L. Glenn and H. W. Leavenworth, Jr., Met.
Prog. Oct. (1984) 19.
- 22.J. Charles, A. Berghezan, A. Lutts and P. L. Dancoisne, Met.
Prog. May (1981) 71.

23. J. C. Garcia, N. Rosas and R. J. Rioja, *Met. Prog.* Aug. (1982) 47.
24. C. N. Hang and T. F. Liu, *Scripta Metall.* 36(8) (1997) 853.
25. C. Y. Chao and T. F. Liu, *Metall. Trans. A.* 24A (1993) 1957.
26. C. Y. Chao and T. F. Liu, *Scripta Metall.* 25 (1991) 1623.
27. C. Y. Chao, C. N. Hwang and T. F. Liu, *Scripta Metall.* 34(1) (1996) 75.
28. S. M. Allen and J. W. Cahn, *Acta Metall.* 24 (1976) 425.
29. S. M. Allen, *Phil. Mag.*, 36(1977) 181
30. P. R. Swann, W. R. Duff and R. M. Fisher, *Metall. Trans. A.* 3 (1972) 409.
31. D. G Morris, M. M. Dadras and M. A. Morris, *Acta Mater.* 41 (1993) 97.
32. 羅亦旋 和 劉增豐, “Phase Transformations in an Fe-8.8Al-30.0Mn-6Cr-1.0C alloy”, 碩士論文.
33. S. Goto, C. Liu, S. Aso and Y. Komatsu, 9th International Conference on Creep & Fracture of Engineering Materials & Structures, 1-4 Apr. (2001) 515.
34. J. Zhang, *Wear.* Vol. 242(1-2) July (2000) 54.

35.H. Vettters and J. M. Schissier, Harterei-Technische Mitteilungen. Vol. 55(3), May-June (2000) 166.

36.Y. Wu and J. D. Lu, Heat Treatment of Metals (China). Vol. 6 June (2002) 34.

37.Y. Wu, J. D. Lu, and L. He, Transactions of Materials and Heat Treatment (China). Vol. 23(2) June (2002). 73

38.William F. Smith, “Structure and properties of Engineering Alloys 2th”

39.C. Y. Chao and C. H. Liu, Materials Transactions. Vol. 43(10) (2002). 2635

